Ceramics-Silikáty 62 (1), 97-107 (2018)
www.ceramics-silikaty.cz doi: 10.13168/cs.2018.0001

# THE EFFECT OF PRESSURE, BIAS VOLTAGE AND ANNEALING TEMPERATURE ON $N_2$ AND $N_2$ + $SiH_4$ DOPED WC/C DC MAGNETRON SPUTTERED LAYERS

PETER HORŇÁK*, **, #DANIEL KOTTFER***, LUKASZ KACZMAREK****, MARTA KIANICOVÁ*, JÁN BALKO**, FRANTIŠEK REHÁK*, MIRIAM PEKARČÍKOVÁ*****, PETER ČIŽNÁR*****

*Alexander Dubček University of Trenčín, Faculty of Industrial Technologies, I. Krasku 491/30, 020 01 Púchov, Slovak Republic
**Slovak Academy of Sciences, Institute of Materials Research, Watsonova 47, 040 01 Košice, Slovak Republic
***Technical University of Košice, Faculty of Mechanical Engineering, Department of Mechanical Technologies and Materials, Mäsiarska 74, 040 01 Košice, Slovak Republic
****Lodz University of Technology, Institute of Materials Science and Engineering, 1/15 Stefanowskiego Str., 90-924 Łódź, Poland
*****Technical University of Košice, Faculty of Mechanical Engineering, Department of Industrial Engineering and Management, B. Němcovej 32, 042 00 Košice, Slovak Republic

#E-mail: daniel.kottfer@tuke.sk

Submitted March 2, 2017; accepted December 29, 2017

**Keywords:** WC/C layer, DC magnetron sputtering, $N_2$ + $SiH_4$, Annealing, Properties

*Tungsten carbide (WC/C) layers are often researched due to their outstanding mechanical and tribological properties. Here, optimized indented hardness ($H_{IT}$), indentation modulus ($E_{IT}$) and coefficient of friction (COF) values were measured to study the effect of pressure and bias voltage on WC/C layers, deposited on Si by DC magnetron spluttering. Maximal values of $H_{IT}$ = 37.2 ± 4.8 GPa, $E_{IT}$ = 447 ± 28 GPa and COF = 0.64 ± 0.09 were obtained. Additionally, the effect of temperature on optimized layers deposited with and without $N_2$ and $N_2$ + $SiH_4$ annealed at 200°C, 500°C and 800°C, were also investigated. The values of $H_{IT}$, $E_{IT}$ and COF and, observed morphology and structural composition of these contaminated and non-contaminated WC/C layers were evaluated. It was found that layer degradation occurred at different rates depending on the temperature and gas mixture used during the annealing and deposition process, respectively.*

## INTRODUCTION

Tungsten carbide (WC) is a very attractive refractory material for industrial applications of thin hard layers to steel [1-12] and Al alloys. WC has an excellent combination of properties, such as high hardness, a high Young's modulus, and a low COF.

Additionally, WC exhibits corrosion and oxidation resistance. It is these characteristics of WC which improve the other properties of materials [13]. WC layers have been deposited using chemical vapor deposition (CVD) [14-22] and physical vapor deposition (PVD) techniques [1-13, 23-31]. Plasma enhanced CVD of tungsten hexacarbonyl has also been used for the deposition of WC/C layers at lower temperatures compared to those used in CVD techniques [15-21].

Carbon occurs in the WC/C layers in the form of *a*-C [8, 9] DLC [8]. WC creates β-$W_2C$ [7, 24] and β-$WC_{1-x}$ [7, 24, 29] phases where the individual forms of C and WC have different indentation of hardness (H), indentation modulus (E) and COF. Various factors which influence the formation of both phases are as follows: the deposited substrate surface temperature [3, 8, 11, 12, 23]; applied pressure and bias voltage [4, 24, 27, 28]; content of carbon in the layers [1, 6, 8, 23]; the flow rate and composition of the precursor [3, 4, 6, 29], and residual stress in the layers [26]. Monocrystalline Si substrate is used to test structural properties under laboratory conditions [27-30].

The abovementioned factors are often evaluated by researchers. Voevodin et al. [23] examined nanocrystalline WC/a-C layers, which produced intersected plasma fluxes when deposition occurred at low temperatures. Hardness equal to 26 GPa was measured. Moreover, Rebholz et al. [1-2] studied a 3μm thick WC/C layer, deposited by the MS technique. Maximal values of $H$ = 40 GPa and $E$ = 300 GPa were reached for a WC layer where there was 15 % carbon content. On the other hand, values of $H$ = 15 GPa a $E$ = 210 GPa were measured for 5 % content of carbon in layer and, the COF value was from 1.0 to 0.7.

Additionally, Wänstrand et al. [3] presented a WC/C layer deposited by the DC MS technique. The carbon phase of the WC/C layer was grown continuously with a hydrocarbon (acetylene, $C_2H_2$) and argon plasma. Gas flow of $C_2H_2$ was varied in range from 100 to 300 $cm^3 \cdot min^{-1}$. Results of the properties for gas flow of 100 $cm^3 \cdot min^{-1}$ have been obtained and they are presented in Table 1.

Likewise, Czyzniewski [6] evaluated WC/C layers in relation to the content of carbon in the layer. Acetylene flow was varied and the maximal value of $H$ = 42 GPa was measured at the concentration of $C$ = 33.7 %. Additionally, $E$ = 460 GPa was obtained at $C$ = 41.3 %.

Furthermore, Palmquist et al. [24] evaluated the concentration dependence of $C$ on 3 phases of WC/C layers, which have been deposited on 3 substrates. $H$, $E$ and COF (Table 1) were evaluated. Maximal values were $H$ = 25 GPa and $E$ = 450 GPa at 35 at. % of $C$. Another technique, XRD, identified a phase mixture of β-$W_2C$ and β-$WC_{1-x}$ at this composition. Weigert et al. [7] also prepared WC layers by reactive and nonreactive DC sputtering. The possibilities of temperature dependence on WC, $WC_{1-x}$ and $W_2C$ phase preparation were investigated. On the other hand, Baragetti et al. [13] used a WC/C layer of 1 μm thickness for studying the influence on fatigue behavior of Al alloy. The hardness of the layer was 10 GPa. Additionally, Shengguo Zhou et al. [9] evaluated nc-WC coating at $C$ = 75 %, and Kosinskiy et al. [10] presented a WC/C layer where $H$ = 6.9 GPa and $E$ = 212 GPa were measured.

Moreover, Novák et al. [26] studied nanohardness of DC magnetron sputtered W/C layers as a function of composition and residual stress. The results obtained were maximal values of $H$ = 19.5 GPa and $E$ = 192 GPa.

Furthermore, Agudelo-Morimitsu et al. [11, 12] presented the WC/C layers deposited within a temperature from RT to 300°C. The values of COF = 0.35 - 0.75, H = 16 - 29 GPa and E = 256 - 448 GPa were measured. Su et al. [27] assessed the influence of bias voltage and annealing temperature on the structural and mechanical properties of WCN layers. Similarly, Gubisch et al. [28] presented WC/C coating deposited by magnetron sputtering in a temperature range from 100°C to 200°C, and a bias voltage in the range from 0 to 200 V. The result H = 19 GPa was obtained.

On the other hand, Pujada and Janssen [30] evaluated hardness of WC:H layers deposited on a Si substrate, by changing the flow of an acetylene precursor. Additionally, Sánchez-López et al. [31] investigated tungsten carbide/amorphous C-based nanocomposite layers for tribological applications. The maximal value of H = 39.6 GPa at C = 39 % and minimal value of COF = 0.19 at C = 72.5 % were found. Parameters of deposition for evaluated layers, as well as the values found for other properties, are shown in the Table 1.

The purpose of this work is to study the effect of pressure and bias voltage on the selected mechanical and tribological properties (COF) of WC/C layers, deposited using the DC magnetron sputtering technique. Furthermore, this work investigates the effect of temperature on the thermal stability, $H_{IT}$, $E_{IT}$ and COF of WC/C layers doped with and without $N_2$ and $N_2$+$SiH_4$. The results obtained are compared to the values reported by the above mentioned authors.

## EXPERIMENTAL

C45 steel (chemical composition of C = 0.42 - 0.50 %, Si max. 0.40 %, Mn = 0.500.80 %, Cr max. 0.40 %, Mo max. 0.10 %, Ni max. 0.40 %, P max. 0.035 %, S max. 0.35 %) was used as substrates for the layer deposition process. Samples were made with wire electrical discharge machining (WEDM) from bars of circular cross-section profile with diameters of 50 and 25 mm. Function areas were produced to the thickness of 3 mm. Substrates were then treated with heat to 860°C and, were kept at a temperature of 200°C. After heat treatment, substrates were polished to the roughness of $R_a$ of ≈ 12 nm. Before deposition, the substrates were cleaned ultrasonically in an acetone environment for 10 minutes, dried with an electric hair drier for 5 minutes

Table 1. Main technological parameters of published WC/C layers and their measured values: $H_{IT}$, $E_{IT}$ and COF.

| Ref. | Deposition technique | Pressure [Pa] | Bias [-V] | Temperature [°C] | Substrate material | Thickness [μm] | $H_{IT}$ [GPa] | $E_{IT}$ [GPa] | COF | % C |
|---|---|---|---|---|---|---|---|---|---|---|
| 1, 2 | DC MS | 0.14 - 0.16 | 50 | 350 | AISI 316 | 3.0 | 15 - 40 | 210 - 300 | 1.0 - 0.7 | 5 - 15 |
| 3 | DC MS | 0.4 - 0.8 | 200 | 200-250 | HSS | 2.0 - 4.0 | 15 - 18 | – | 0.35 | – |
| 6 | MS | 0.3 - 0.4 | 100 | 150 | Steel 100Cr6 | 3.0 - 3.5 | 14 - 42 | 140 - 460 | – | 31.8 -95.5 |
| 7 | DC MS | 3.0 | – | 450 | Stainless Steel | 1.5 | – | – | – | – |
| 9 | DC MS | $10^{-3}$ | 300 | – | Stainless Steel | 2.1 | 24 | 281 | 0.12 | 75 |
| 10 | MS | 0.85 | 0 | 25 | 90MnCrV8 steel | 0.4 | 6.9 | 212 | 0.2 - 0.3 | – |
| 11 | DC MS | – | – | 25, 100, 200, 300 | AISI 316 | up to 0.9 | – | – | – | 21 - 27 |
| 12 | DC MS | – | – | 25, 100, 200, 300 | AISI 316 | up to 0.9 | 16 - 29 | 256 - 448 | 0.35 - 0.75 | – |
| 13 | MS | – | – | 180 | 2011-T6 Al alloy | 1.0 | 10.0 | – | – | – |
| 23 | – | – | – | 45 - 300 | – | – | – | – | – | – |
| 24 | DC MS | 0.2 | 300-350 | 450 | $Al_2O_3$ | 0.5 | 14 - 25 | 300 - 450 | – | 22 - 45 |
| 26 | DC MS | 0.25 | – | – | – | 0.6 | 16 - 19.5 | 179 - 192 | – | – |
| 27 | DC MS | – | 0-200 | – | Si | – | 32 - 47 | – | – | – |
| 28 | MS | 0.85 | 0-200 | 100 - 200 | Si | 0.21 | 19 | – | – | – |
| 31 | MS | $3 \times 10^{-4}$ | – | 150 - 200 | M2 steel | 1.5 - 2.0 | 15.8 - 39.6 | – | 0.19 -0 .84 | 34 - 72.5 |

and, then cleaned in the Ar glow discharge for 15 minutes. Si substrates with thickness of 1.0 mm were used to study the high temperature effect on oxide resistance of WC/C layers, deposited using DC magnetron sputtering (MS) technique.

Stoichiometric WC target (97 %, 90 mm in diameter) was used for the deposition process. Target-to-substrate distance was kept constant at 10 cm. The molecules from the target were ionized in Ar (99.999 % purity) glow discharge and, accelerated toward the substrate with the negative substrate bias voltage varying from 0 V to -500 V during magnetron sputtering. Additional deposition parameters considered were the total gas pressure in the chamber, which was in range from 0.2 Pa to 2 Pa, and the negative bias on the samples' holder ($U_b$), which was in the range from 0 V to -500 V (Table 2). Pressure, bias and current are shown in the Table 2. Deposition parameters were: target power = 175 W (350 V, 0.5 A); current intensity = 2.75 $W \cdot cm^{-2}$; target chemical content = WC; target coil current = 1.5 A; deposition time was 180 min and 90 min. The temperature was varied between 200°C and 250°C.

With respect to the surface morphology, thickness and microstructures of the layers were evaluated by scanning electron microscopy (SEM) JEOL 7000F with EDX detector. Chemical content was evaluated as an in-depth concentration GDOES profile. Surface roughness ($R_a$) was measured by confocal microscopy: Plu Neox, Sensofar, Spain and, atomic force microscopy: Dimension Icon, Veeco, USA.

Instrumented indentation hardness ($H_{IT}$) and indentation modulus ($E_{IT}$) of the layers were measured using nanoindenter: NHT with Berkovich tip, CSM Instruments, Switzerland. The sinus mode of 15 Hz with amplitude of 1 mN and, the indentation load in the range from 20 mN to 60 mN were used in relation to the thickness of the layer. Every value means the arithmetic mean value of the peak achieved from 20 nanoindentation load-displacement curves. Curves with extreme behavior were excluded from analyses.

The coefficient of friction (COF) was investigated by means of a Ball-on-disc method, using a tribometer: HTT, CSM Instruments, Switzerland. The following parameters were used: normal load = 0.5 N, rotation speed = 10 $cm \cdot s^{-1}$, wear track = 50 m, room temperature = 23°C. As a counterpart, the 100Cr6 steel ball with diameter 6 mm was used. Layers deposited with the addition of gases were evaluated by the nanotribometer, using CSM NTR2 Flat-on-disc method. The following parameters were used: indentation load = 0.5 N, frequency = 10 Hz, wear track = 50 m, room temperature = 23°C. As a counterpart, the 100Cr6 steel ball with diameter 2 mm was used. Wear of solved layers and ball counterpart were not evaluated.

Phase content of WC/C layers was measured by X-ray diffraction analysis using X´Pert PRO Philips with high-speed linear detector (X´Celerator) in the Bragg-Brentano parafocusing arrangement with angular correlation of θ/2θ. A copper source was used ($I$ = 40 kV, $U$ = 50 mA) with characteristic CuKα 1,2 X-rays and, a corresponding wavelength of 1.54 Å. X-ray diffraction patterns were measured in the range from 10° to 100° and, step size of 0.033°. Qualitative analysis was done by the CMPR program – a powder diffraction toolkit [32]. Evaluation of experimental results was performed by comparing the values obtained to a powder diffraction file (PDF-2) database.

Annealing of WC/C layers was performed in an electric furnace without protected (controlled) atmosphere at 200°C, 500°C and 800°C. Annealing time took 1 hour and samples were cooled to room temperature.

## RESULTS AND DISCUSSION

In the first part of the research, the deposition parameters were chosen so that maximal value of hardness and minimal value of COF were reached. The pin-on-disc test was performed and, COF was evaluated. The second part included deposition of WC/C layers using the parameters which were used to achieve the maximal hardness and Young's modulus, so that $N_2$ was flowing into the vacuum chamber during deposition of the layer. Additionally, $N_2$+$SiH_4$ were flowing into the vacuum chamber during the subsequent deposition process to obtain the layer doped by Si. $H_{IT}$, $E_{IT}$ and COFs were measured for all these layers. Finally, samples were annealed at 200°C, 500°C and 800°C and, $H_{IT}$, $E_{IT}$ and *COF* were measured so that phases for the layer could be evaluated.

### Influence of deposition parameters on hardness and indentation modulus

At the first optimization phase, the suitable pressure in vacuum chamber was identified on the basis of results ($H_{IT}$ and $E_{IT}$) obtained under different pressure. Deposition range was from 0.1 Pa to 1.0 Pa. Influence of total pressure on indentation $H_{IT}$ and $E_{IT}$ can be seen in Figure 1a. The constant negative bias ($U_b$ = 170 V) was used on holder of washer. Both dependences showed that the total $H_{IT}$ and $E_{IT}$ tended to noticeable decrease at a pressure which is greater than 0.2 Pa. The lowest values of $H_{IT}$ and $E_{IT}$ were at a pressure of 0.5 Pa where, an increase of the investigated parameters occurred again. Based on the fact mentioned above, the pressure of 0.2 Pa was determined as optimal with respect to maximal hardness achieved.

In Table 2, technological parameters and mechanical properties (such as $H_{IT}$, $E_{IT}$ and *COF*) are shown. Subsequently, the optimization of a negative bias voltage ($U_b$) was specified. The whole specification process was similar to that of the optimization process in the previous case with respect to the selected parameters. This

is because a constant pressure of 0.2 Pa in the vacuum chamber was selected.

Additionally, bias voltage ($U_b$) was in the range from 0 V to -500 V. The influence of bias voltage on the hardness and Young's modulus can be seen in the Figure 1b. Bias voltage in the range from -170 V to -220 V was determined to be optimal. Maximum values of optimized hardness of WC/C layers were 37.2-37.8 GPa (Figures 1, 2) at a bias voltage of -170 V and pressure of 0.2 Pa. Moreover, *COF* was 0.64 and 0.67.

Table 2. Deposition parameters and measured properties of evaluated layers, respectively.

| Sample No. | Pressure [Pa] | Bias [-V] | Current [A] | $H_{IT}$ [GPa] | $E_{IT}$ [GPa] | COF |
|---|---|---|---|---|---|---|
| 1 | 1 | 0 | 0 | 17 ± 1.5 | 308 ± 25.9 | 0.26 |
| 2 | 0.5 | 100 | 0.03 | 21.7 ± 1.7 | 320 ± 16.6 | 0.34 |
| 3 | 0.2 | 170 | 0.03 | 37.8 ± 5.5 | 488 ± 48.3 | 0.64 |
| 4 | 0.5 | 500 | 0.4 | 18.1 ± 1.2 | 270 ± 12.6 | 0.81 |
| 5 | 0.2 | 170 | 0.03 | 37.2 ± 4.8 | 447 ± 28 | 0.67 |
| 6 | 0.2 | 300 | 0.04 | 33.9 ± 3.2 | 440 ± 17.3 | 0.37 |
| 7 | 0.1 | 170 | 0.03 | 29.5 ± 2.6 | 377 ± 11.2 | 0.77 |
| 8 | 0.3 | 170 | 0.03 | 20.7 ± 1.4 | 318 ± 17.8 | 0.65 |
| 9 | 0.3 | 420 | 0.03 | 24.3 ± 2.2 | 319 ± 23 | 0.70 |
| 10 | 0.2 | 250 | 0.04 | 36.5 ± 7.6 | 441 ± 45.8 | 0.72 |
| 11 | 0.2 | 500 | 0.04 | 18.6 ± 0.8 | 256 ± 17.2 | 0.65 |

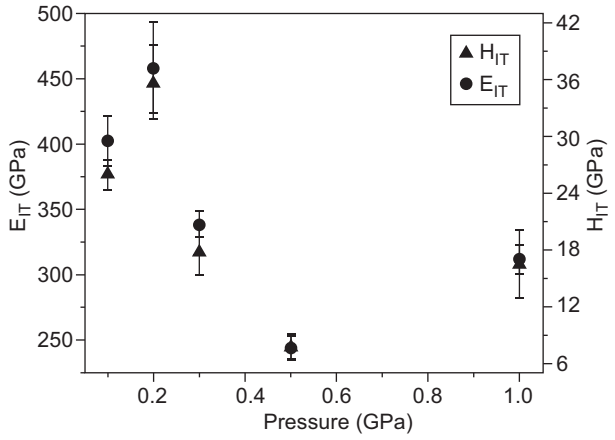


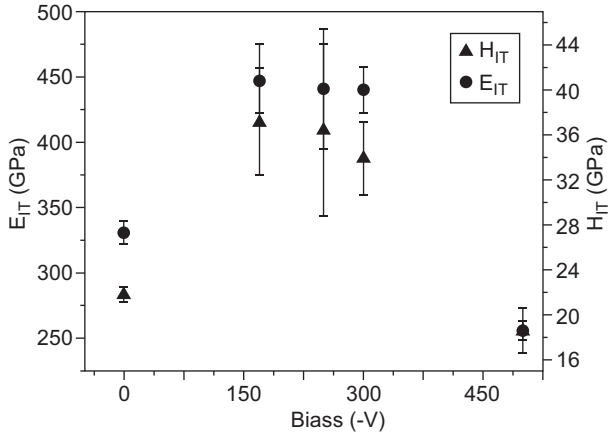


Figure 1. Influence of: a) pressure on $H_{IT}$ and $E_{IT}$ ($U_b$ = -170 V); b) bias on $H_{IT}$ and $E_{IT}$ (pressure = 0.2 Pa).

Firstly, Palmquist et al. [24] used the same pressure but bias voltage was from -300 V to -350 V and, hardness was in the range (14-25) GPa. This is less by 30-50 % compared to our values. COF was not measured.

Secondly, Rebholz and co-authors [1, 2] used a pressure similar to former but bias was -50 V. Their measured value of $H_{IT}$ was 40 GPa and, this is in good conformity with our values. Moreover, their minimal value of COF is also similar to our result. On the other hand, the maximal value of COF is higher by 30 %.

Thirdly, Wänstadt et al. [3] reached hardness of 15 GPa and even 18 GPa at pressures of 14 Pa and 16 Pa, respectively. This is lower by 30 % compared to our values but, COF was similar to our value. It becomes apparent that not only bias, but also pressure and even temperature of deposition, have an influence on hardness. Owing to this fact, the hardness depends on the content of hard WC phase in the layer.

Furthermore, Abad et al. [8] investigated WC/C coating sputtered on M2 steel with a WC underlayer which, was deposited by sputtering the WC target at 250 W while the substrates were negatively biased with a direct current source at 100 V. The layer had the following maximal values: $H$ = 40 GPa, $E$ = 520 GPa and *COF* = 0.8 at 3 % content of a-C, and these values obtained are more by about 10% compared to our values. In fact, COF was higher by 20 % compared to our value.

On the other hand, minimal values, including $H$ = 16 GPa, $E$ = 270 GPa and *COF* = 0.2 were in good conformity with our values. These values were measured at 33 % content of a-C. This indicates that $H_{IT}$, $E_{IT}$ and *COF* depend on *C* content in the a-C form. When the *C* content in the a-C form is higher, the *COF* and $H$ are lower.

## Influence of deposition parameters on COF

The next step was to find deposition parameters of the WC/C layer with respect to the minimal value of COF. Table 2 shows COF data for individual depositions. The original values of COFs have increased from 0.1 - 0.25 to 0.3 - 0.7 at a distance of 10 m (Figure 2). In the case of sample 2, with mean value of hardness HIT ≈ 22 GPa, the lowest COF = 0.3 was achieved along a track over 30 m and, this is in good correspondence with previous investigations [3, 10, 12, 31].

As far as the technological parameters of deposition are concerned, we can say that chamber pressure has an effect on the final hardness and COF. This was confirmed by Wänstrand et al. [3], because they achieved COF = = 0.3 at pressure near 0.4 Pa. This result is in the good

conformity with sample 2. On the other hand, authors [13] have measured the lowest value of hardness compared with our value, representing 16.7 GPa. Based on the comparison of $H_{IT}$, as well as COF, it is evident that the lowest value of COF = 0.34 was obtained in the case of sample 2 (Figure 2). To the contrary, the layers exhibited the higher values of the hardness.

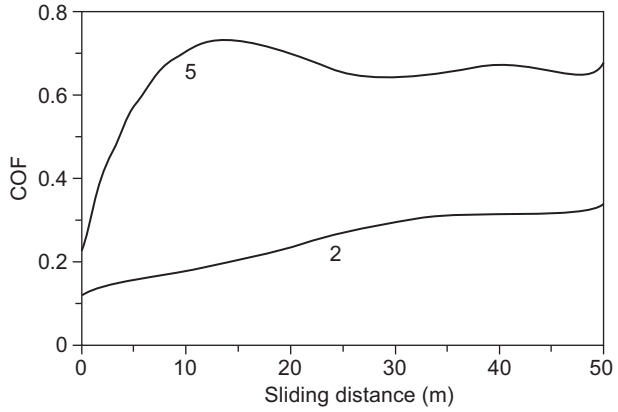


Figure 2. COF maximum and minimum of WC/C layers.

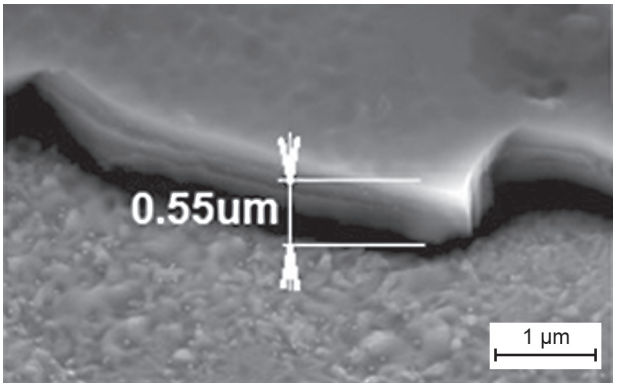


a)

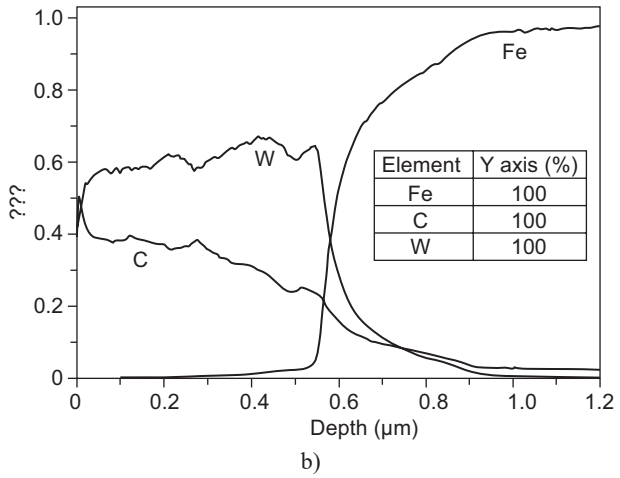


b)

Figure 3. a) Thickness (SEM); b) GDOES profile of WC/C layer.

## Thickness, chemical content and microstructure of WC/C layer

Morphology, thickness and chemical composition of the deposited layer was presented on Figures 3a and b, respectively. Figure 4 shows the regularly structured surface of WC/C layer with roughness of $S_a = 20 \pm 2$ nm. The thickness of the layer was 0.55 µm (Figure 3a) and, this was confirmed by the GDOES method (Figure 3b).

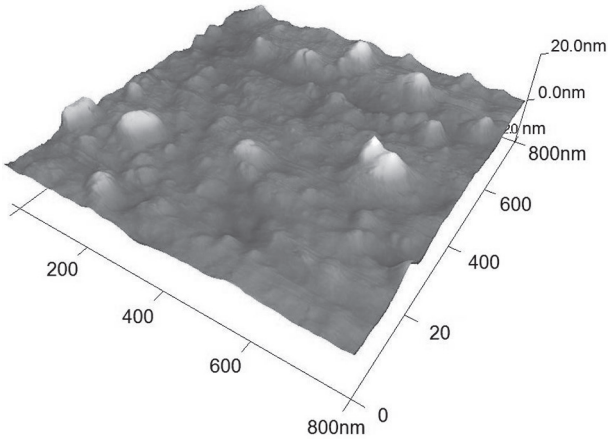


Figure 4. Roughness (AFM) of WC/C layer – $S_a = 20 \pm 2$ nm.

## Effect of additive gases and temperature of annealing

In the previous part, the optimization of WC/C layers in the Ar environment without additive gases was reported to reach the highest hardness. Maximal hardness was achieved in the Ar additive gas environment, with relatively high COF. Next step was to achieve oxidation resistance of WC/C layers by addition $SiH_4$ gas during coating deposition. $SiH_4$ is an explosive gas and, for this reason, it was used in 1.5 vol. % in a mixture of $N_2$+$SiH_4$. In this phase of optimization, silane depositions were done by DC magnetron sputtering. During deposition, the parameters achieved in the first part of the experiment were used. The aim was to keep maximal values of hardness with respect of COF changes. Maximal values are shown in Table 3.

Table 3. $H_{IT}$, $E_{IT}$ and COF of WC layers with and without additive gases.

| Additional gas | $H_{IT}$ (GPa) | $E_{IT}$ (GPa) | COF |
|---|---|---|---|
| – | 37.2 ± 4,8 | 447 ± 28 | 0.64 ± 0.09 |
| $N_2$ | 18.1 ± 1.7 | 235 ± 20 | 0.46 ± 0.07 |
| $N_2$ + $SiH_4$ | 24.5 ± 1.2 | 278 ± 22 | 0.44 ± 0.08 |

*Influence of argon*

*Morphology* (Figure 5) – Notably, the surface of the sample is smooth, and the structure in the cross section at RT has amorphous character. The thickness of the layer is 0.6 μm (Figure 5d). Globular particles, oxides of W (see arrows) become visible after annealing at 500°C. They have diameter up to 0.4 μm. Dark areas (Figure 5b) show starting points of layer disruption. After annealing at 800°C, changes occur in the structure. On the surface, globular particles of oxides and nitrides of tungsten, with diameter up to 0.4 μm are visible (Figures 5c, e). There is rupture in the structure as a result of the swelling process – relating to the second phase, where $O_2$ (penetrating the layer) reacts with C and W [33] to produce $CO_2$ and $WO_3$, respectively.

*Phase analysis* – layer phase analysis (Figure 6) verified the occurrence of the carbide $WC_{1-X}$ phase (ICDD ref. code: 00-020-1316). After heat treatment at 500°C, $WC_{1-X}$ did not exhibit decomposition to the other kinds of phases and this is in compliance with Abad et al. [8]. Further annealing at 800°C caused the $WC_{1-X}$ phase to transform into $W_2C$ and WC phases (ICDD ref. codes: 00-035-0776 and 00-072-0097, respectively). There was also formation of $WO_2$ and $WO_3$ oxides (ICDD ref. code: 00-032-1393 and 00-020-1323, respectively) in the layer. The formation of $W_2N$ and $WN_2$ nitrides (ICDD ref. codes: 00-025-1257 and 00-075-0998, respectively) were the result of the annealing temperature. The other $W_2Si$ phase (ICDD ref. code: 00-011-0195) occurred due to a reaction between the substrate and layer.


a)

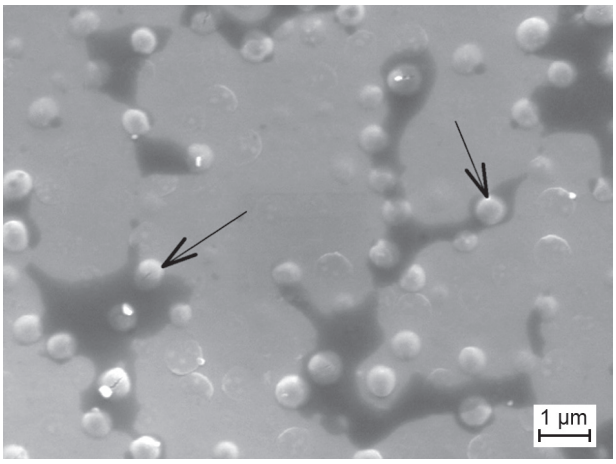


b)

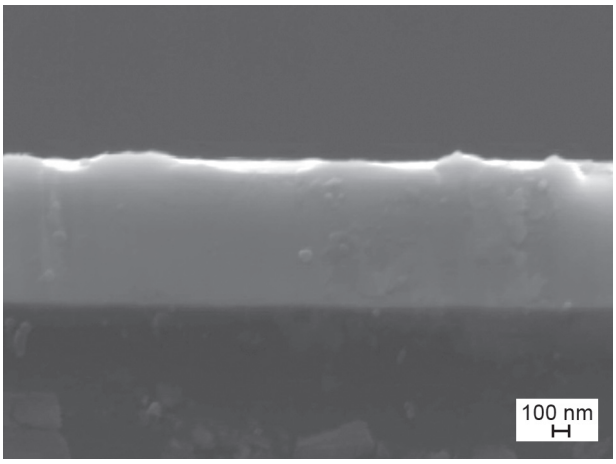


d)

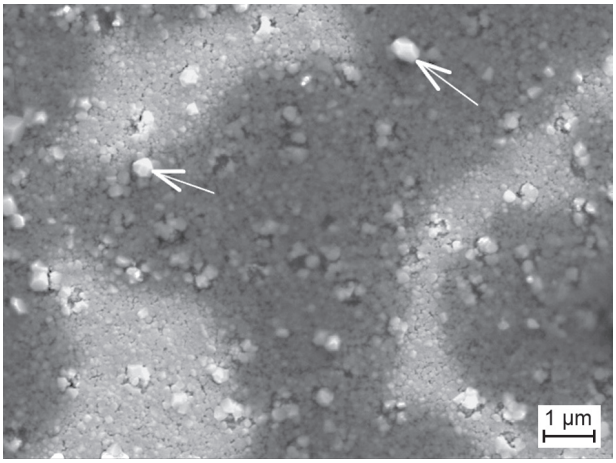


c)

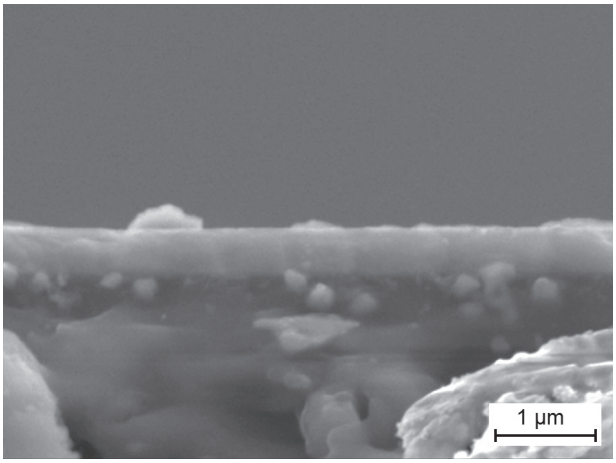


e)

Figure 5. Front view and cross sectional view of the WC layer: a), d) RT and annealed at: b), e) 500°C, c) 800°C.

*Mechanical properties and COF – $H_{IT}$* and *COF* of WC/C layers, in compliance with annealing temperature, with and without doped gases, are visible in Figure 7. The COF value at RT, measured by the fretting method, is lower by 50 % compared to the value obtained by the flat-on-disc method.

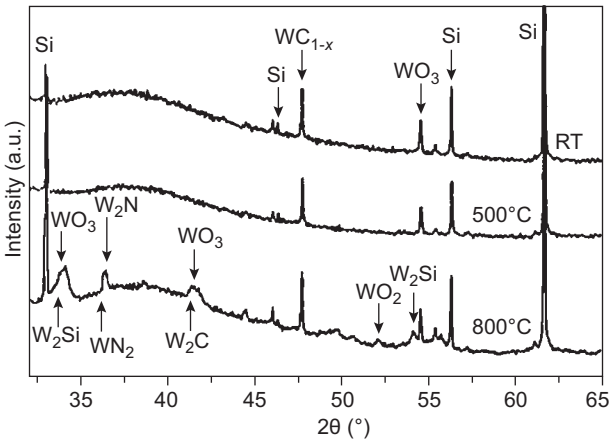


Figure 6. X-ray diffraction scans of WC layers at RT, after annealing at 500°C and 800°C; Si phase (ICDD ref. code: 00-027-1402).

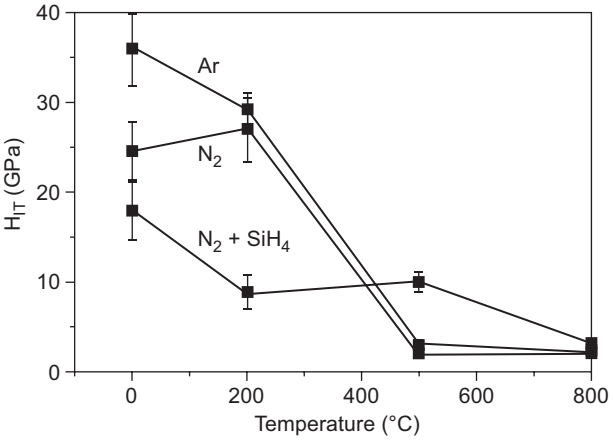


a)

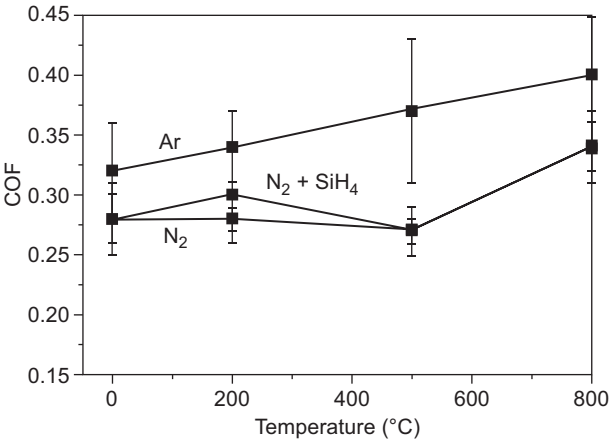


b)

Figure 7. Dependence of $H_{IT}$ (a) and COF (b) on annealing temperature of WC/C layers with and without doping gases.

*Effect of $N_2$*

*Morphology* – the layer surface is smooth. In the cross-section, the evidence of columns is visible and hence, the layer exhibits amorphous character. Layer thickness is up to 0.7 µm (Figures 8a, d). After annealing at 500°C, there is a visible change of the surface due to the oxidation process and, empty areas from 0.2 µm up to 1.0 µm occur in the layer (Figure 8b) [33]. The cross-section shows the occurrence of two sublayers; an upper sublayer which has thickness nearly 0.2 µm and a lower carbide sublayer nearly 0.4 µm thick (Figure 8e). Nonetheless, the amorphous character of the layer is maintained. After annealing at 800°C, significant damage can be seen. Areas without the layer reach 40 %. On the coated surface, WO particles with size of 1.0 µm are present (see arrows on the Figure 8c). This problem can be attributed to the oxygen penetrating from the environment to the surface of the layer where oxygen subsequently reacts with carbon. The result of this reaction relates to the formation of $CO_2$, which rises

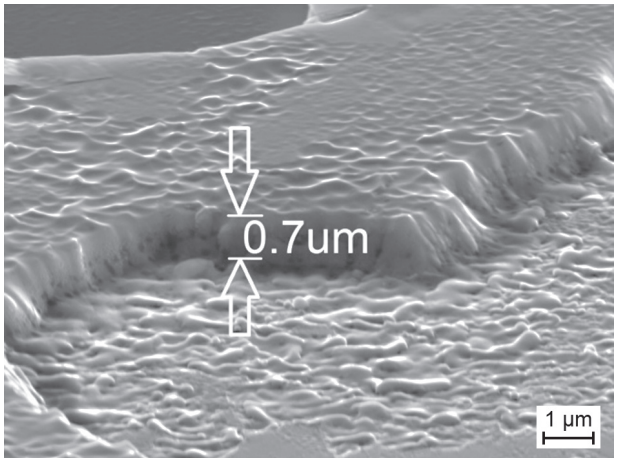


a)

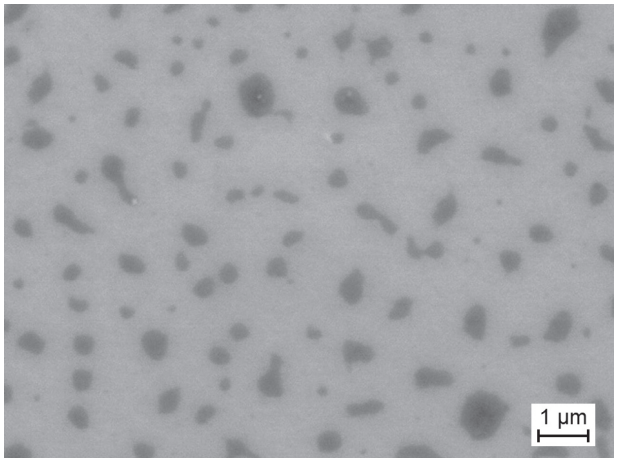


b)

Figure 8. Front view and cross sectional view of the WC layer doped with N2: a), d) at RT; b), e) annealed at 500°C; c) annealed at 800°C. *(Continue on next page)*

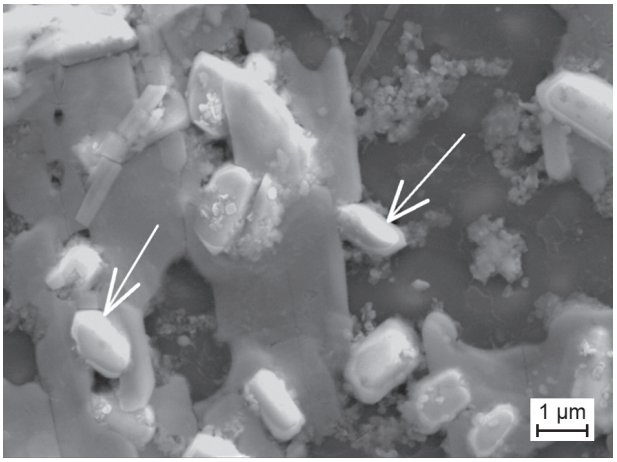


c)

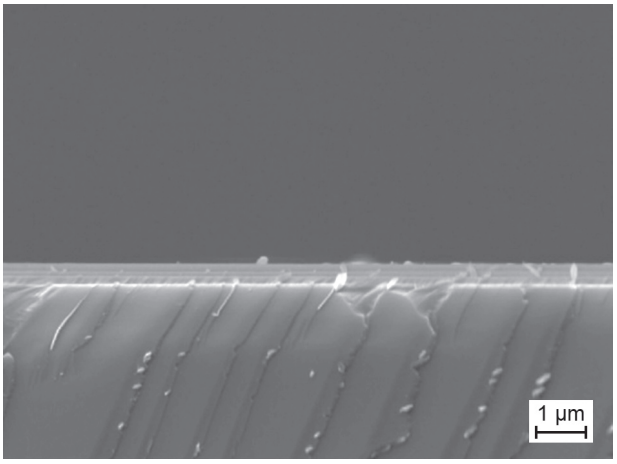


d)

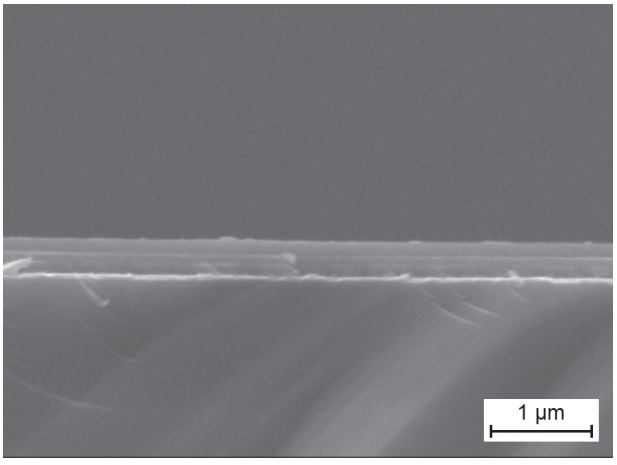


e)

Figure 8. Front view and cross sectional view of the WC layer doped with N2: a), d) at RT; b), e) annealed at 500°C; c) annealed at 800°C.

from the layer and, it leads to the noticeable disruption of the layer [33] (Figure 8c). There is also the occurrence of layer spalling from the substrate.

*Structure analysis* – phase analysis of WC/C coating at RT and, of the annealing temperature (500°C) does not show the crystal character of the layer. Decomposition of $WC_{1-X}$ (ICDD ref. code: 00-020-1316) to other types of phases does not occur and, this is in the agreement with Abad et al. [8]. Annealing at 800°C begins the formation of oxide phases, such as $WO_2$, $WO_3$ and $W_2N$ (ICDD ref. code: 00-032-1393, 00-020-1323 and 00-025-1257, respectively) – Figure 9.

*Mechanical properties* – $H_{IT}$ at RT is 24.5 ± 1.2 GPa. However, annealing at 200°C caused $H_{IT}$ to increase to 27 GPa but, annealing at 500°C caused $H_{IT}$ to decrease to 12 GPa. Annealing at 800°C also led to $H_{IT}$ declining to 3 GPa (Figure 7a). The value of *COF* = 0.27 is constant at all temperatures (RT, 200°C and 500°C), and annealing at 800°C caused the COF to increase to 0.33 (Figure 7b). From these values, we can declare that the $N_2$ additive was the reason for decreasing the value of *COF* up to 20 % with respect to the layer without gas additives.

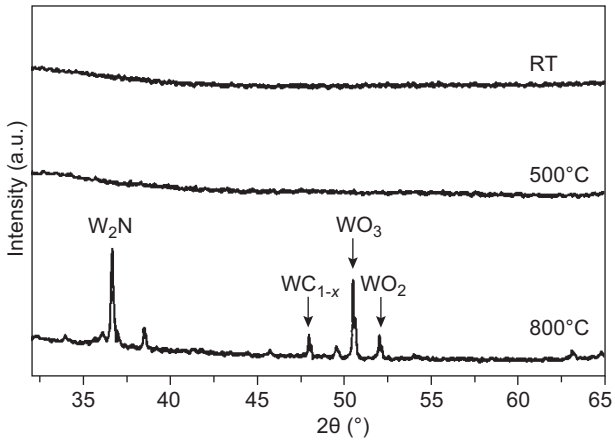


Figure 9. X-ray diffraction scans of WC layer doped with $N_2$ at RT, after annealing at 500°C and 800°C.

Effect of $N_2$+$SiH_4$ mixture

*Morphology* – surface coating without annealing exhibited a structure typical of globular shape, with diameter of 100 nm (Figure 10a). The thickness of the coating is 1.6 µm (Figure 10d). Additionally, oxide particles were not present in the coating. However, annealing at 500°C caused grain coarsening and, the surface globular particles became larger (Figure 10b – see arrows). The cross-section shows the column character of the layer and, the occurrence of two sublayers; an upper sublayer which has thickness nearly 2 µm and a lower carbide sublayer nearly 1 µm thick (Figure 10e). This may be due to the oxidation process and $CO_2$ formation, which tends to rise from the layer surface, leading to the increased of thickness, as well as subsequent disruption, of the layer [33].

Grains were coarser from 0.2 up to 0.5 µm (Figure 10c) due to annealing at 800°C. Moreover, the lower sublayer lost its columnar structure (Figure 10f), and the upper oxide sublayer became porous due to swelling caused by the temperature change [33]. Nonetheless, its thickness is almost the same as it was after annealing at 500°C.

*Phase structure* – phase analysis of the WC/C layer at RT (Figure 11) proved the presence of a $WC_{1-x}$ phase (ICDD ref. code: 00-020-1316). Notably, annealing at 500°C caused layer decomposition and, the formation of $W_2C$ phase (ICDD ref. code: 00-0201315) and oxide phases in the form of $WO_2$ and $WO_3$ (ICDD ref. codes: 00-032-1393 and 00-020-1323, respectively) were observed. Further annealing up to 800°C led to the extinction of carbide phase $WC_x$ (ICDD ref. code: 00-020-1314) and, the formation of $WO_2$ and $WO_3$ oxides (ICDD ref. codes: 00-032-1393 and 00-020-1323, respectively) throughout the whole deposited layer.

*Mechanical properties* (Figure 7) – H at RT was 18 GPa, but it decreased to 8 GPa after annealing at 200°C.

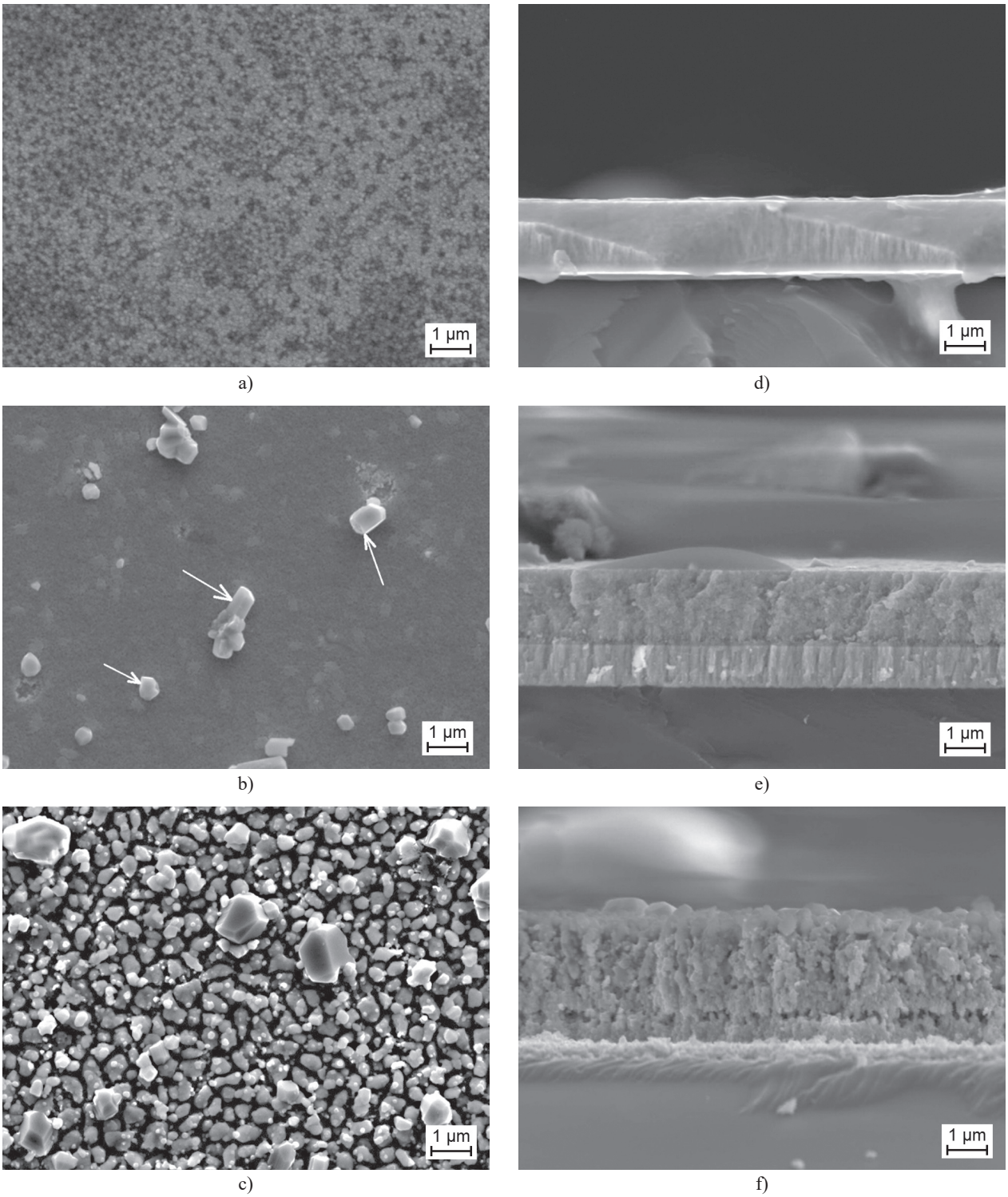


Figure 10. Front view and cross sectional view of the WC/C layer doped with $N_2$ + $SiH_4$: a), d) without annealing; b), e) annealed at 500°C; c), f) annealed at 800°C.

Subsequently, it increased to 10 GPa after annealing at 500°C (Figure 7a). This effect can be caused by coarsening the layer, with its amorphous character of upper sublayer and oxides inside of it. Below this sublayer, the coating is most likely composed of carbide particles. Moreover, annealing at 800°C caused a decline in hardness to 3 GPa. The course of *COF* is identical to that which was characteristic for the $N_2$ additive doping. Consequently, the $N_2$ gas additive had a similar effect to the $N_2$+$SiH_4$ gas additive mixture because they both decreased COF. On the other hand, the $N_2$ gas additive decreased $H_{IT}$ at RT after annealing at 200°C, but increased $H_{IT}$ after annealing at 500°C (Figure 7b).

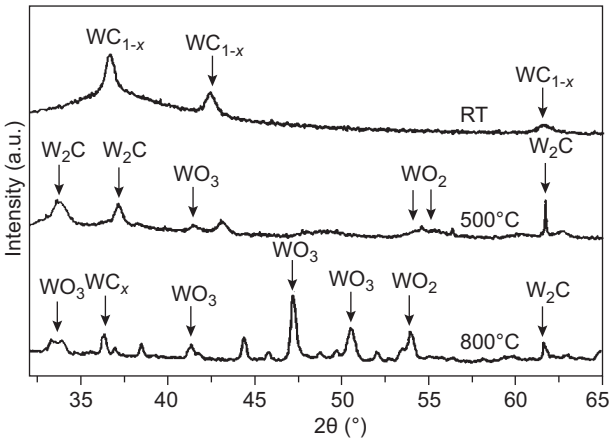


Figure 11. X-ray diffraction scans of WC layer doped with $N_2$ + + $SiH_4$ at RT, after annealing at 500°C and 800°C.

## CONCLUSIONS

Using predetermined technological parameters, the WC/C layer deposited by DC magnetron sputtering, was evaluated in order to find the maximal value of $H_{IT}$. Mechanical properties such as $E_{IT}$ and COF were also evaluated. Additionally, the effect of temperature and doping gases during the deposition process on the mechanical and tribological properties and, WC/C phase composition were evaluated.

We can draw the following conclusions:

- Maximal values were: $H_{IT}$ = 37.2 - 37.8 GPa, $E_{IT}$ = 488 ± 48.3 GPa with a bias voltage of -170 V and pressure of 0.2 MPa. On other hand, the values of *COF* were 0.64 and 0.67,
- Additive gases such as $N_2$ and $N_2$+$SiH_4$ markedly increased the values of $H_{IT}$,
- The annealing temperature decreased $H_{IT}$ of the layer deposited in the presence of $N_2$. Values of $H_{IT}$ after annealing were close to $H_{IT}$ values without $N_2$ being present,
- In the case of the layer deposited with the $N_2$ + $SiH_4$ mixture of gases, the value of $H_{IT}$ experienced a less dramatic decrease under the influence of annealing. Notably, the mixture of these gases had a significant effect on the *COF*; values of *COF* decreased by 25 % at RT in comparison with the layer deposited without gas additives. An annealing temperature up to 500°C did not have any effect on the *COF* but the temperature of 800°C caused a significant increase in the *COF* value,
- During the annealing process in unprotected atmosphere, the coating degraded due to oxidation which was accompanied by the swelling of the layer. Additive gas $N_2$ slowed down layer degradation at 500°C; under the condition of an annealing temperature of 800°C, layer disruption was hugely significant and, spalling of the layer was observed. Furthermore, the mixture of $N_2$ +$SiH_4$ gases reduced oxidation – swelling and layer degradation up to 800°C did not show layer spalling,
- To improve the oxidation resistance of WC/C layers deposited by DC magnetron sputtering, it is appropriate to use additive gases such as $N_2$,
- In the process of sputtering the compound $SiH_4$ was added as a reactive gas in the form of the mixture $N_2$+$SiH_4$. During the deposition a constant pressure of the gas mixture was kept in the vacuum chamber. In the dependence of plasma conditions, one could expect reactions leading to a creation of $WSi_2$, SiC, $SiO_2$ and $Si_3N_4$ compounds. The effect of plasma conditions on the creation of these compounds will be a subject of further research which could be also interesting with respect to the influence of the silane partial pressure in the deposition process.

### Acknowledgments

*This work was financially supported by the Slovak Grant Agency grant numbers VEGA 1/0432/17, 1/0117/15, 1/0708/16 and KEGA 030TUKE-4/2017 and APVV-15-0710.*

## REFERENCES

1. Rebholz C., Schneider J.M., Ziegele H., Rähle B., Leyland A., Matthews A. (1998): Deposition and characterisation of carbon-containing tungsten layers prepared by reactive magnetron sputtering, *Vacuum, 49*, 4, 265-272. doi: 10.1016/S0042-207X(98)00122-5
2. Rebholz C., Schneider J.M., Leyland A., Matthews A. (1999): Wear behaviour of carbon-containing tungsten layers prepared by reactive magnetron sputtering, *Surface and Coatings Technology*, *112*, 85–90. doi: 10.1016/S0257-8972(98)00786-5
3. Wänstrandt O., Larsson M., Hedenqvist P. (1999): Mechanical and tribological evaluation of PVD WC/C layers, *Surface and Coatings Technology*, *111*, 247–254. doi: 10.1016/S0257-8972(98)00821-4
4. Esteve J., Zambrano G., Rincon C., Martinez E., Galindo H., Prieto P. (2000): Mechanical and tribological properties of tungsten carbide sputtered layers, *Thin Solid Films*, *373*, 282-286. doi: 10.1016/S0040-6090(00)01108-1

5. Rincón C., Romero J., Esteve J., Martíinez E., Lousa A. (2003): Effects of carbon incorporation in tungsten carbide films deposited by r.f. magnetron sputtering: single layers and multilayers, *Surface and Coatings Technology*, *163–164*, 386–391. doi: 10.1016/S0257-8972(02)00635-7
6. Czyzniewski A. (2003): Deposition and some properties of nanocrystalline WC and nanocomposite WC/a-C:H layers, *Thin Solid Films, 433*, 180–185. doi: 10.1016/S0040-6090 (03)00324-9
7. Weigert E.C., Humbert M.P., Mellinger Z. J., Ren Q., Beebe Jr. T. P., Bao L., Chen J.G. (2008): Physical vapor deposition synthesis of tungsten monocarbide (WC) thin films on different carbon substrates, *Journal of Vacuum Science Technology A*, *26*, 23-28. doi: 10.1116/1.2806941
8. Abad M.D., Muñoz-Márquez M.A., El Mrabet S., Justo A., Sánchez-López J.C. (2010): Tailored synthesis of nanostructured WC/a-C layers by dual magnetron sputtering, *Surface and Coatings Technology, 204*, 3490–3500. doi: 10.1016/j.surfcoat.2010.04.019
9. Zhou S.G., Wang L., Wang S.C., Xue Q. (2011): Comparative study of simplex doped nc-WC/a-C and duplex doped nc-WC/a-C(Al) nanocomposite layers, *Applied Surface Science*, *257*, 6971–6979. doi: 10.1016/j.apsusc.2011.03.045
10. Kosinskiy M., Ahmed S.I.U, Liu Y., Gubisch M., Mastylo R., Spiess L., Schaefer J.A. (2011): Friction and Wear Properties of WC/C Nano-Scale Multilayer Layers on Technical Surfaces, *Tribology Letters*, *44*(1), 89-98. doi: 10.1007/s11249-011-9826-2
11. Agudelo-Morimitsu L.C., DeLaRoche J., Escobar D., Ospina R., Restrepo-Parra E. (2013): Substrate heating and post-annealing effect on tungsten/tungsten carbide bilayers grown by non-reactive DC magnetron sputtering, *Ceramics International*, *39*, 7355–7365. doi: 10.1016/j.ceramint.2013.02.075
12. Agudelo-Morimitsu L.C., DeLaRoche J., Ruden A., Escobar D., Restrepo-Parra E. (2014): Effect of substrate temperature on the mechanical and tribological properties of W/WC produced by DC magnetron sputtering, *Ceramics International, 40*, 7037–7042. doi: 10.1016/j.ceramint.2013.12.033
13. Baragetti S., Lusvarghi L., Bolelli G., Tordini F. (2009): Fatigue behaviour of 2011-T6 aluminium alloy coated with PVD WC/C, PA-CVD DLC and PE-CVD SiOx layers, *Surface and Coatings Technology*, *203*, 3078–3087. doi: 10.1016/j.surfcoat.2009.03.040
14. Neto M.A., Silva E.L., Fernandes A.J.S., Oliveira F.J., Silva R.F. (2011): Deposition of alpha-WC/a-C nanocomposite thin films by hot-filament CVD. *Surface and Coatings Technology*, 206, 103–106. doi: 10.1016/j.surfcoat.2011.06.049
15. Sun Y.-M., Lee S.Y., Lemonds A.M., Engbrecht E.R., Veldman S., Lozano J., White J.M., Ekerdt J.G., Emesh I., Pfeifer K. (2001): Low temperature chemical vapor deposition of tungsten carbide for copper diffusion barriers. *Thin Solid Films,* 397, 109. doi: 10.1016/S0040-6090(01)01367-0
16. Ferdinandy M., Lofaj F., Dusza J., Kottfer D. (2011): Preparation of Nanocrystalline WC Layers by Plasma Enhanced CVD-PVD Employing $W(CO)_6$ Decomposition (in slovak). *Chemické listy-Chemical letters*, 105, 442 – 444.
17. Lofaj F., Ferdinandy M., Kottfer D., Dusza J., Němeček J. (2009): Tribological Properties of the Cr-C and W-C Based PECVD Nanocomposite Layers, in: *Proceedings of the 11th ECERS Conference*, Krakow.
18. Lofaj F., Mikula M., Grančič B., Cempura G., Horňák P., Kúš P., Kottfer D. (2011): Tribological properties of $TiB_x$ and WC/C layers, *Ceramics – Silikáty*, 55, 4, 305-311.
19. Lofaj F., Ferdinandy M., Cempura G., Horňák P., Vnouček M. (2013): Transfer Film in a Friction Contact in the Nanocomposite WC-C Layers, *Journal of the Australian Ceramic Society*, 49, 1, 34–43.
20. Lofaj R., Ferdinandy M., Cempura G., Dusza J. (2012): Nanoindentation, AFM and tribological properties of thin nc-WC/a-C Layers, *Journal of the European Ceramic Society*, *32*, 2043–2051. doi: 10.1016/j.jeurceramsoc.2012.01.037
21. Kelly C.M., Garg D., Dyer P.N. (1992): Kinetics of chemical vapor deposition of tungsten carbide, *Thin Solid Films*, *219*, 103–108. doi:10.1016/0040-6090(92)90729-U
22. Wessbecher Skaf D., Warner A.W., Dollahon N.R., Fargo G.H. (1994): Microstructure and properties of CVD tungsten carbide from tungsten hexafluoride and dimethyl ether, *Materials Characterization,* 33, 393–402. doi: 10.1016/1044-5803(94)90144-9
23. Voevodin A.A., O'Neill J.P., Prasad S.V., Zabinski J. S. (1999): Nanocrystalline WC and WC/a-*C*WC/a-C composite layers produced from intersected plasma fluxes at low deposition temperatures, *Journal of Vacuum Science Technology A, 17*, 986-992. doi: 10.1116/1.581674
24. Palmquist J.-P., Czigany Zs., Odén M., Neidhart J., Hultman L., Jansson U. (2003): Magnetron sputtered W-C films with C60 as carbon source, *Thin Solid Films, 444*, 29–37. doi: 10.1016/S0040-6090(03)00937-4
25. El Mrabet S., Abad M.D., Sánchez-López J.C. (2011): Identification of the wear mechanism on WC/C nanostructured layers, *Surface and Coatings Technology*, *206*, 1913–1920. doi: 10.1016/j.surfcoat.2011.07.059
26. Novák M., Lofaj F., Hviščová P., Podoba R., Haršáni M., Sahul M., Čaplovič Ľ. (2015): Nanohardness of DC Magnetron Sputtered W – C Layers as a Function of Composition and Residual Stresses, *Key Engineering Materials*, *662*, 107-110. doi: 10.4028/www.scientific.net/KEM.662.107
27. Su Y.D., Hu C.Q., Wen M., Wang C., Liu D.S., Zheng W.T. (2009): Effects of bias voltage and annealing on the structure and mechanical properties ofWC0.75N0.25 thin films, *Journal of Alloys and Compounds, 486*, 357–364. doi: 10.1016/j.jallcom.2009.06.147
28. Gubisch M., Liu Y., Spiess L., Romanus H., Krischok S., Ecke G., Schaefer J.A., Knedlik Ch. (2005): Nanoscale multilayer WC/C layers developed for nanopositioning: Part I. Microstructures and mechanical properties, *Thin Solid Films, 488*, 132 – 139. doi: 10.1016/j.tsf.2005.04.107
29. Abdelouahdi K., Sant C., Legrand-Buscema C., Aubert P., Perrière J., Renou G., Houdy Ph. (2006): Microstructural and mechanical investigations of tungsten carbide films deposited by reactive RF sputtering, *Surface and Coatings Technology*, *200*, 6469–6473. doi: 10.1016/j.surfcoat.2005.11.015
30. Pujada B.R., Janssen G.C.A.M. (2006): Density, stress, hardness and reduced Young's modulus of W–C:H layers, *Surface and Coatings Technology*, *201*, 4284–4288. doi: 10.1016/j.surfcoat.2006.08.058
31. Sánchez-López J.C., Martínez-Martínez D., Abad M.D., Fernández A. (2009): Metal carbide/amorphous C-based nanocomposite layers for tribological applications, *Surface and Coatings Technology*, *204*, 947–954. doi: 10.1016/j.surfcoat.2009.05.038
32. Toby B.H. (2005): CMPR – a powder diffraction toolkit, *Journal of Applied Crystallography*, *38*, 1040-1041. doi: 10.1107/S0021889805030232
33. Lofaj F., Kaganowskyy Yu.S. (1995): Kinetics of WC-Co oxidation accompanied by swelling, *Journal of Material Science, 30*, 1811-1817. doi: 10.1007/BF00351615